Proceedings of the Tenth Pacific Conference on Earthquake Engineering
Building an Earthquake-Resilient Pacific
6-8 November 2015, Sydney, Australia

# Seismic performance comparison of linear and nonlinear viscous dampers in base-isolated buildings

E. Güler & C. Alhan

*Department of Civil Engineering, İstanbul University, Avcılar, İstanbul*

**ABSTRACT:** Improved protection of buildings against detrimental effects of earthquakes can be achieved by seismic isolation. However, the near-fault earthquake challenge, described by the possibility of the coincidence of high-amplitude long-period velocity pulses with the isolation periods of buildings that may result in large base displacements leading to the rupture and/or buckling of isolators, is still a major concern and supplemental damping provided by linear or nonlinear viscous dampers has been suggested against such catastrophic failures previously. While use of nonlinear viscous dampers instead of linear ones may be a better alternative in reducing base displacements under near-fault earthquakes, its potential drawbacks, i.e. possibility of amplified superstructure response under far-fault earthquakes, are yet to be examined. Here, this issue is numerically investigated by comparing the seismic performances, i.e. base displacements, top floor accelerations, and roof drift ratios of benchmark six-story base-isolated buildings equipped with (i) linear viscous dampers, (ii) nonlinear viscous dampers, and (iii) no dampers under far-fault and near-fault earthquakes. Findings have revealed that while use of nonlinear viscous dampers is more effective in reducing isolator displacements under near-fault earthquakes in comparison to use of linear ones, it may result in significant amplifications in the superstructure response.

## 1 INTRODUCTION

Seismic isolation systems can effectively reduce both floor accelerations and inter-story drift ratios (Komodromos 2000). However, in case of near-fault earthquakes, these systems can be threatened by very large base displacements (Hall et al. 1995, Heaton et al. 1995, Alhan and Altun 2009) which can be successfully reduced via use of supplemental dampers at the isolation system (Hall and Ryan 2000, Providakis 2008, Mazza and Vulcano 2009, Providakis 2009). Although most research studies existing in the literature concentrated on linear viscous dampers rather than nonlinear ones, Tsopelas et al. (1994) were the ones to present a case study which shows that nonlinear viscous dampers may reduce the base displacements more efficiently. However, they have not evaluated the comparative performance of the superstructure, which may reveal inadvertent effects of the use of nonlinear supplemental viscous dampers on the superstructure response. In order to shed light to this issue, in this study, we investigate the efficiency of nonlinear supplemental viscous dampers with respect to the linear ones in terms of seismic response parameters including base displacements, top floor accelerations, and roof drift ratios. A numerical investigation under far-fault and near-fault earthquakes is carried out using a benchmark six-story base-isolated building equipped with (i) linear viscous dampers, (ii) nonlinear viscous dampers, and (iii) no dampers.

## 2 STRUCTURAL MODEL

### 2.1 Superstructure

In this parametric study, a six-story superstructure (Alhan and Sürmeli 2011) is used. The three dimensional view of the moment resisting reinforced concrete frame superstructure (benchmark building with fixed-base condition) is given in Figure 1. Cross-sectional dimensions of all beam and column elements are 45 cm × 45 cm and 30 cm × 55 cm, respectively with an elasticity modulus of 32000 MPa. All floors are modelled as rigid diaphragms with three degrees of freedom at each floor: two translational and one rotational. Superstructure is fully symmetric with modal damping ratios of 5% for all modes and 0.68 s translational periods. The natural period, eigenvalues, and eigenvectors of the superstructure is obtained via a modal analysis in SAP2000 (CSI 2011) which is then used as part of the input generated for the base-isolated building model in 3D-BASIS-ME (Tsopelas et al. 1994).

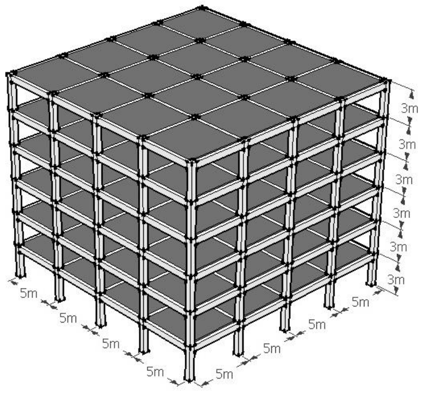


Figure 1: Three dimensional view of the superstructure

### 2.2 Isolation system

In the base-isolated model, a rigid base floor is defined at the base level with an isolation system underneath it composed of high damping rubber bearings placed under each column along with supplemental dampers. Three different isolation systems are considered by using (i) linear viscous dampers, (ii) nonlinear viscous dampers, and (iii) no dampers.

#### 2.2.1 *Isolators*

Hysteretic nonlinear behaviour of the high damping rubber bearings are defined using smooth bi-linear fore-deformation relationship. The parameters which characterise an isolation system composed of such rubber bearings are the pre-yield stiffness ($K_1$), the post-yield stiffness ($K_2$), the characteristic force ($Q$), the yield force ($F_y$), the ratio of characteristic force $Q$ to the total building weight $W$ ($Q/W$), and the yield-displacement ($D_y$). In this context, with $M$ being the total mass (including base floor) of the base-isolated building, post-yield isolation period ($T_0$) and post-yield angular frequency ($\omega_0$) is given by (Nagarajaiah et al. 1991):

$$T_0 = \frac{2\pi}{\omega_0} \tag{1}$$

$$\omega_0 = \sqrt{\frac{K_2}{M}} \tag{2}$$

In order to represent a typical base-isolated building, the post-yield period is assumed to be $T_0$ = 3s which yields $K_2$ = 9825.74 kN/m using Equations (1) and (2). For a typical post-yield to pre-yield stiffness ratio of $K_2 / K_1$ = 0.1 and a yield displacement of $D_y$ = 10 mm, the pre-yield stiffness and the yield force are calculated as $K_1$ = 98257.39 kN/m and $F_y = K_1 \times D_y$ = 982.57 kN, respectively. Then the characteristic force can be obtained by (Naeim and Kelly 1999)

$$K_1 - K_2 = \frac{Q}{D_y} \tag{3}$$

that results in $Q$ / $W$ = 4 % which falls in the range of typical characteristic force ratios used in design of base-isolated buildings.

#### 2.2.2 *Supplemental Dampers*

Supplemental viscous dampers are placed in parallel with the isolators as part of the base isolation system. The behaviour of a viscous damper can be defined as follows (Tsopelas et al. 1994):

$$F_D = c \times V_D^{\alpha} \tag{4}$$

where $c$, $F_D$, $V_D$ and $\alpha$ represents viscous damping coefficient, damper force, relative velocity of damper, and velocity exponent which describes the level of nonlinearity attaining values typically between 0.5 and 1.2 (Constantinou and Symans 1992), respectively. For $\alpha$ = 1.0 the damper is a linear viscous damper.

The total viscous damping coefficient (C), assuming linear viscous damping, can be calculated by

$$C = 2 \times \zeta \times M \times \omega_0 \quad (5)$$

where $\zeta$ is the supplemental damping ratio based on the post-yield angular frequency ($\omega_0$) which is considered as $\zeta$ = 20 % in this study. The total damping coefficient is calculated via this methodology and divided by the number of dampers to find the viscous damping coefficient of a single damper as $c$ = 75.06 kNs/m. In case of nonlinear viscous dampers, a nonlinear velocity exponent of $\alpha$ = 0.5 is assumed and the damping constant is adjusted such that the damper forces are equivalent to the linear ones under the design earthquake LGP000 for which peak damper velocities are equal to 1.234 m/s.

## 3 EARTHQUAKE DATA

Two historical earthquake records, representing a near-fault and a far-fault earthquake are used to test the benchmark base-isolated buildings. The records are obtained from Berkeley University PEER Ground Motion Database (Berkeley, 2013). LGP000 component of the 1989 Loma Prieta earthquake recorded at the LGPC station and I-ELC180 component of the 1940 Imperial Valley earthquake recorded at the El Centro station represents near-fault and far-fault earthquakes, respectively. Information on these records is presented in Table 1.

**Table 1. Characteristics of the earthquake records.**

| Component | Record Date | The Closest Distance To The Fault (km) | Moment Magnitude (-) | Peak Ground Acceleration (g) | Peak Ground Velocity (cm/s) | Peak Ground Displacement (cm) |
|---|---|---|---|---|---|---|
| LGP000 | 10/18/1989 | 6.1 | 7.1 | 0.563 | 94.8 | 41.18 |
| I-ELC180 | 05/19/1940 | 8.3 | 7.2 | 0.313 | 29.8 | 13.32 |

Velocity time histories of the ground motions are shown in Figures 2a and 2b. Typical near-fault earthquake records contain long-period high-amplitude velocity pulses (Sommerville 1998, He and Agrawal 2008) and LGP000 record is a near-fault earthquake record as shown Figure 2a. Peak ground velocity of I-ELC180 record is relatively small and does not contain a velocity pulse (Fig. 2b), bearing properties of a typical far-fault earthquake record.

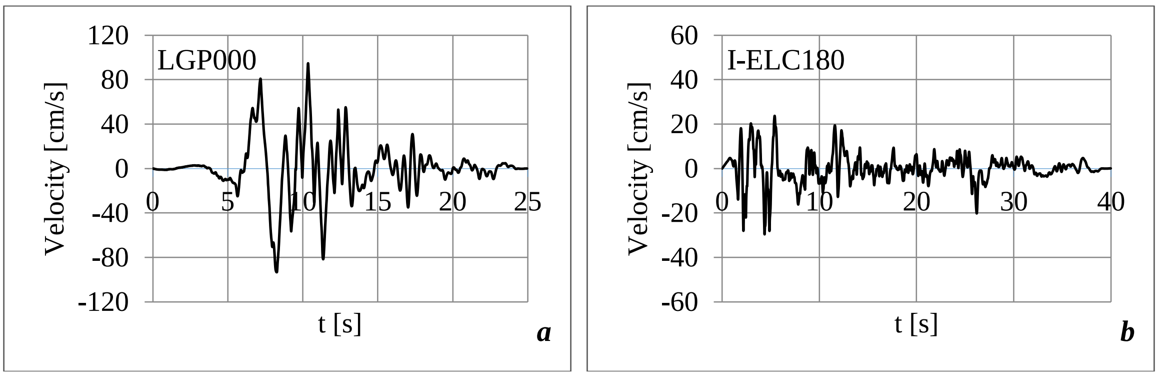


Figure 2: Velocity time histories of the ground motions

The acceleration and displacement response spectra (20 % damped) for the unidirectional records are also given in Figures 3a and 3b, respectively. In particular, it is clearly seen that the near-fault LGP000 record results in much larger displacements at the isolation period range.

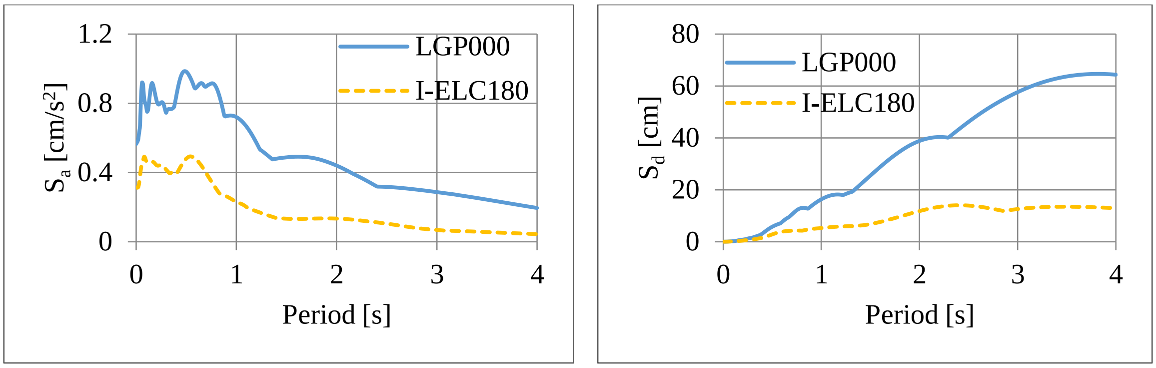


Figure 3: 20 % damped acceleration response spectra and displacement response spectra

## 4 DISCUSSION OF RESULTS

Time history plots of base displacements ($d$), top floor accelerations ($a$), and roof drift ratios ($\varDelta$) are given in Figures 4 and 5 for LGP000 and I-ELC180 earthquake records, respectively. These figures include plots corresponding to three cases: (i) isolation system with nonlinear viscous dampers of velocity exponent $\alpha$ = 0.5 and $\zeta$ = 20 %, (ii) isolation system with linear viscous dampers ($\alpha$ = 1.0) and $\zeta$ = 20 %, and (iii) no additional dampers ($\zeta$ = 0 %).

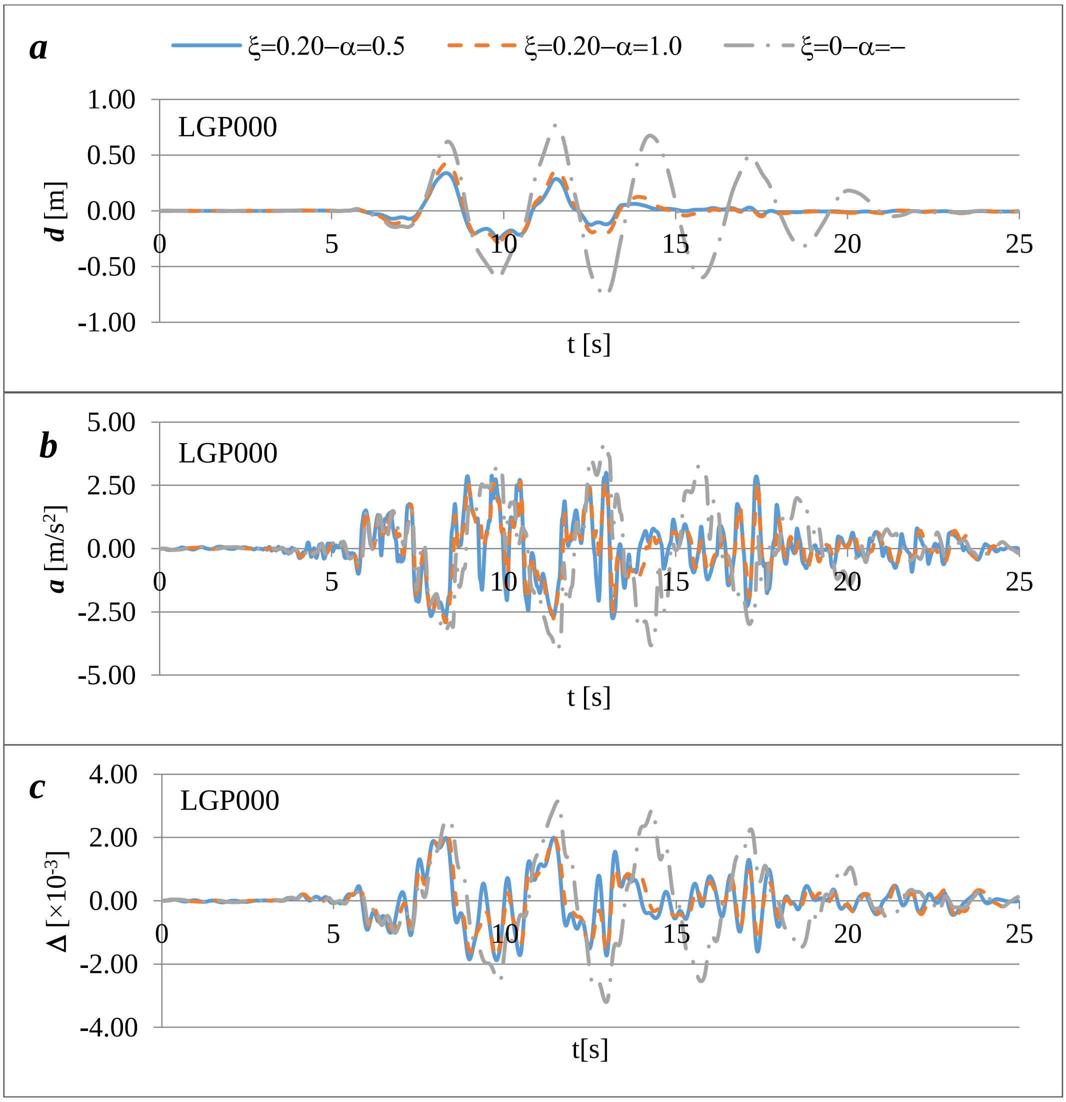


Figure 4: Base displacement (a), top floor acceleration (b), and roof drift ratio (c) responses for LGP000 record

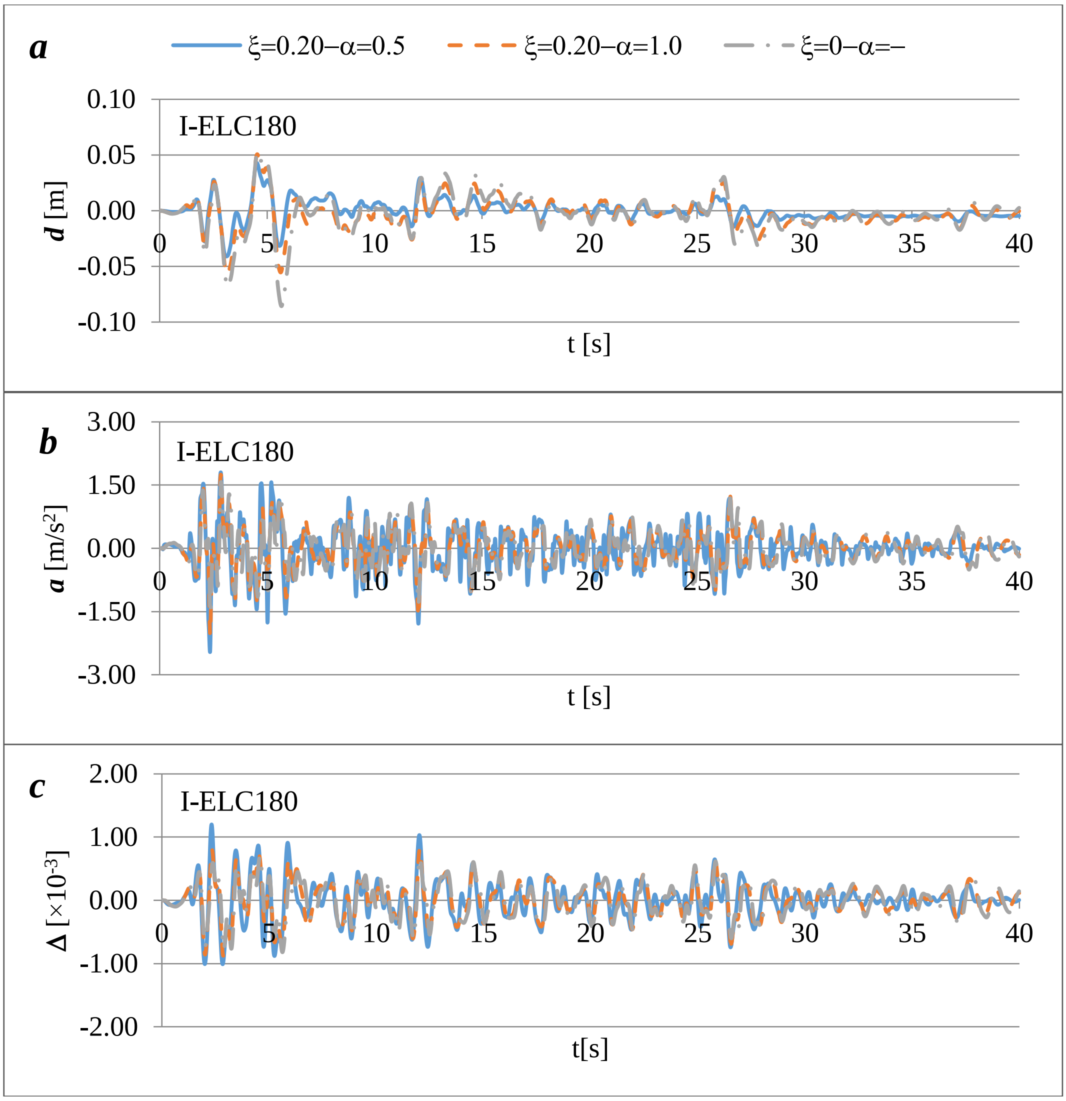


Figure 5: Base displacement (a), top floor acceleration (b), and roof drift ratio (c) responses for I-ELC180 record

The difference in the time histories between three cases can be clearly observed from the time histories but in order to make a quantitative comparison, peak values of the aforementioned structural responses are presented also for all cases and earthquakes in a comparative fashion in Figure 6.

As seen in Figure 6a, in case of no additional damper (only with hysteretic damping provided by the rubber isolators), peak base displacement goes up to 76.69 cm for the near-fault LGPC000 record which is rather a high value. Through use of supplemental linear viscous dampers, the peak base displacement is reduced down to 42.64 cm. And, use of nonlinear viscous dampers results in a peak base displacement of 33.92 cm which is 20 % less compared to linear viscous damper case. This extra reduction in peak base displacements could be very valuable in case of near-fault earthquakes. On the other hand, for I-ELC180 record, the peak base displacement value is already low (8.56 cm) with no supplemental dampers. Thus, providing supplemental damping is in fact unnecessary even though it reduces peak base displacements further down to 5.69 cm and 4.29 cm in case of linear and nonlinear viscous dampers, respectively (Fig. 6b). Note that, in this study we intentionally do not scale up the far-fault I-ELC180 record which would increase the base displacement demand. Because, we are specifically interested in observing the behaviour of the benchmark building under relatively weak far-fault records when the building is already provided with supplemental damping that is required for handling the strong near-fault record of LGPC000.

As seen in Figure 6c, use of linear viscous dampers reduces peak top floor acceleration from 4.15 $m/s^2$ down to 2.92 $m/s^2$ for LGPC000 record. The result is approximately the same when nonlinear dampers are used where an insignificant increase to 3.00 $m/s^2$ is observed. A similar behaviour is observed in terms of peak roof drift ratio response. As seen in Figure 6e, use of linear viscous dampers reduces peak roof drift ratio from 3.20 × $10^{-3}$ down to 2.13 × $10^{-3}$ for LGPC000 record. The result is approximately the same when nonlinear dampers are used where an insignificant decrease to 2.00 × $10^{-3}$ is observed.

Floor acceleration and story drift responses portray a completely different tendency under far-fault earthquake record I-ELC180. We see a negative effect of the use of supplemental dampers, particularly the nonlinear ones. As seen in Figure 6d, use of supplemental linear viscous dampers causes an increase in the top floor acceleration from 1.58 m/s$^2$ to 2.07 m/s$^2$. Use of nonlinear viscous dampers instead of linear ones further worsens the situation by causing an even higher acceleration value of 2.47 m/s$^2$. Likewise, use of supplemental linear viscous dampers causes an increase in the peak roof drift ratio from 0.82 × $10^{-3}$ to 0.88 × $10^{-3}$. Use of nonlinear viscous dampers instead of linear ones further worsens the situation by causing an even higher drift ratio value of 1.20 × $10^{-3}$ (Fig. 6f).

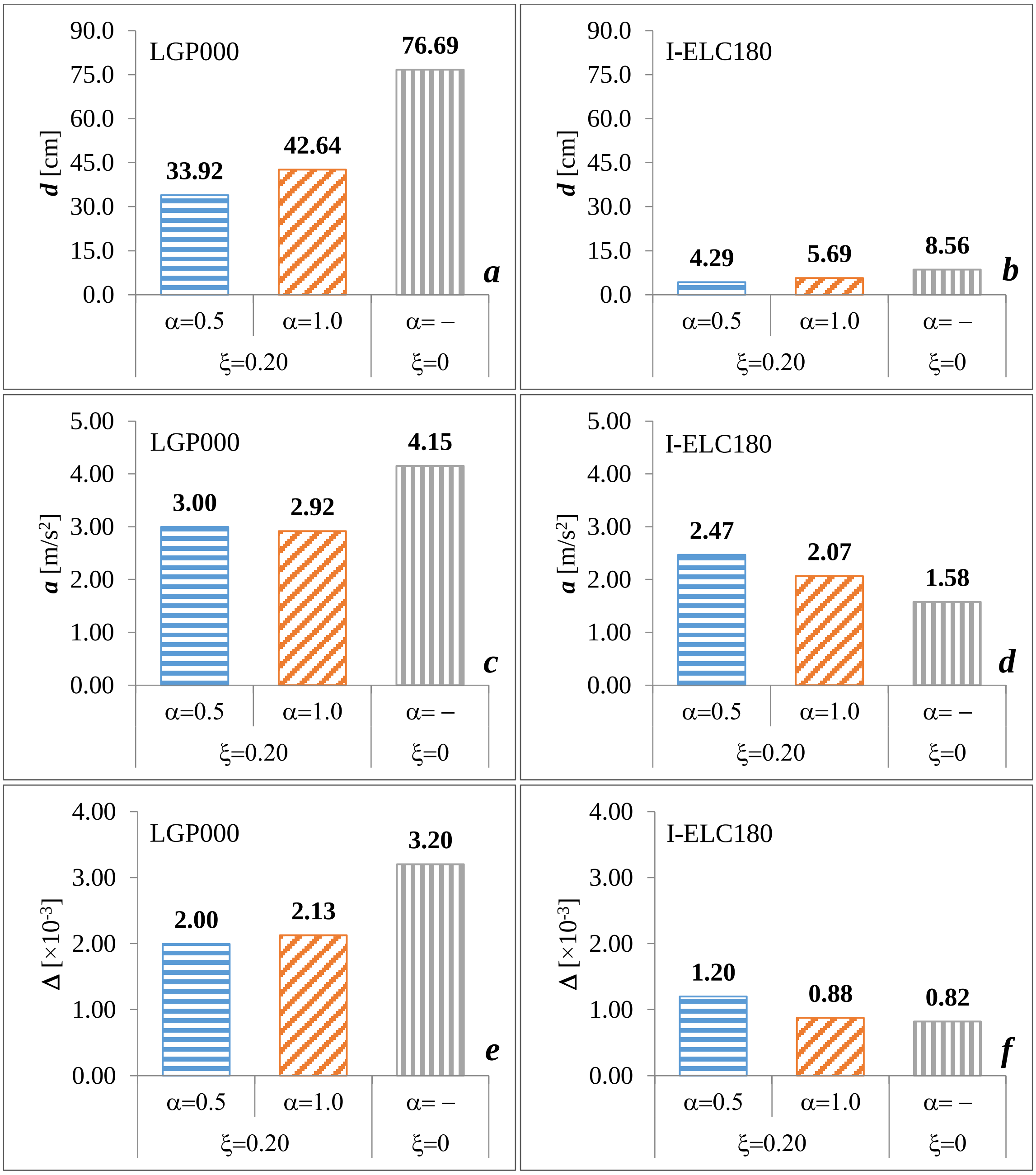


Figure 6: Peak base displacement (a, b), peak top floor acceleration (c, d), and peak roof drift ratio (e, f) responses for LGP000 and I-ELC180 records

For a direct comparison of the seismic performances of seismic isolation systems equipped with linear and nonlinear supplemental viscous dampers, “ratios of peak values” are calculated by dividing the peak responses obtained for nonlinear dampers case by the responses obtained for linear dampers case. **P**eak **B**ase **D**isplacement **- R**atio (***PBD-R***), **P**eak **T**op **F**loor **A**cceleration **- R**atio (***PTFA-R***) and **P**eak **R**oof **D**rift **R**atio **- R**atio (***PRDR-R***) values are presented in Figure 7a and 7b for LGP000 and I-ELC180 records, respectively. As seen in these figures for both LGP000 and I-ELC180 records peak base displacements are further reduced (20% and 25%) via use of nonlinear viscous dampers instead of linear ones. However, while peak top floor acceleration and peak roof drift ratio responses nearly remained the same for near-fault LGP000 record (i.e. peak top floor acceleration is increased by 3% and peak roof drift ratio is decreased by 6%), the very same responses are significantly increased for far-fault I-ELC180 record (i.e. peak top floor acceleration and peak roof drift ratio are increased by 20% and 37%, respectively) via use of nonlinear viscous dampers instead of linear ones.

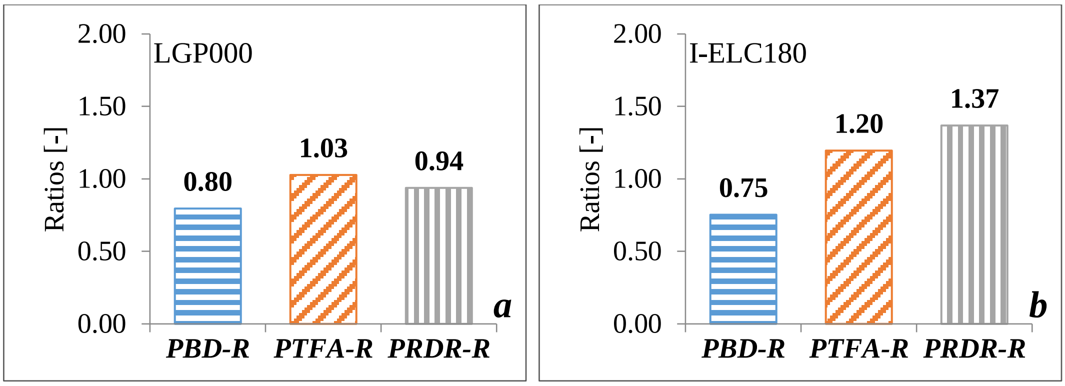


Figure 7: Ratios of peak responses (responses from nonlinear dampers case divided by the response from linear dampers case) for LGP000 (a) and I-ELC180 (b) records

In order to identify the efficiency of using supplemental damping compared to hysteretic damping only (i.e. where no supplemental damping is used), the ratios of peak base displacements, peak top floor accelerations, and peak roof drift ratios are calculated by dividing the responses obtained for supplemental damper cases by the responses obtained for no supplemental dampers case and given in Table 2. As seen in this table, all responses are reduced via use of supplemental damping in case of near-fault earthquake LGP000. However, peak top floor accelerations and peak roof drift ratio responses are amplified when supplemental damping (linear or nonlinear) is used in case of far-fault I-ELC180 earthquake although peak base displacements are reduced.

**Table 2. Ratios of peak structural responses for LGP000 and I-ELC180 records.**

| | Ratios Of Peak Base Displacements (-) | | Ratios Of Peak Top Floor Accelerations (-) | | Ratios Of Peak Roof Drift Ratios (-) | |
|---|---|---|---|---|---|---|
| Linearity Exponent (-) | LGP000 | I-ELC180 | LGP000 | I-ELC180 | LGP000 | I-ELC180 |
| 0.5 | 0.44 | 0.50 | 0.72 | 1.56 | 0.62 | 1.46 |
| 1.0 | 0.56 | 0.66 | 0.70 | 1.31 | 0.66 | 1.07 |

## 5 CONCLUSIONS

In this study, efficiency of the use of nonlinear viscous supplemental dampers in comparison to use of linear ones and use of no additional dampers are investigated via nonlinear time history analyses of a benchmark base-isolated building subjected to far-fault and near-fault earthquakes. Based on the results of this investigation, following conclusions are drawn:

- While linear supplemental viscous dampers reduce base displacements under near and far-fault earthquakes, the nonlinear ones provide further reduction which would be particularly useful in avoiding very large base displacements that may occur in near-fault earthquakes.

- Floor accelerations and story drift ratios are significantly reduced via use of supplemental viscous dampers under near-fault earthquakes. And the degree of reduction is about the same for nonlinear and linear ones.
- Floor accelerations and story drift ratios may significantly increase due to use of supplemental viscous dampers under far-fault earthquakes. And in case of using nonlinear ones, this amplification in the superstructure response may be worse compared to using linear ones.
- In order to effectively deal with large base displacements realized under near-fault earthquakes, isolation systems need to be equipped with nonlinear dampers rather than linear ones. But then, superstructure performance may worsen under far-fault earthquakes.

## ACKNOWLEDGMENTS

This work was supported by Scientific Research Projects Coordination Unit of Istanbul University. Project number UDP-55219 and BAP-19354.

## REFERENCES:

Alhan, C. & Altun, M. 2009. Performance of non-linear base isolation systems designed according to uniform building code. *5th Intl. Advanced Technologies Symposium*, 13-15 May 2009, 2079-2084, Karabük, Turkey.

Alhan, C. & Sürmeli, M. 2011. Shear building representations of seismically isolated buildings. *Bulletin of Earthquake Engineering*, 9 (5), 1643-1671.

Berkeley, 2013. http://ngawest2.berkeley.edu/, *Peer Ground Motion Database* [Visit Date: 06 May 2015].

Constantinou, M.C. & Symans, M.D. 1992. Experimental and analytical investigation of seismic response of structures with supplemental fluid viscous dampers. *Technical report NCEER-92-0032*. National center for earthquake engineering research, State University of New York at Buffalo, New York.

CSI, 2011. *SAP2000 Structural Analysis Program: Static and dynamic finite element analysis of structures*, V15.1. Berkeley, USA: Computers and Structures Inc.

Hall, J.F., Heaton, T.H., Halling, M.W., Wald, D.J. 1995. Near-source ground motion and its effects on flexible buildings. *Earthquake spectra*, 11 (4), 569-605.

Hall, J.F. & Ryan, K.L. 2000. Isolated buildings and the 1997 UBC near-source factors. *Earthquake spectra*, 16 (2), 393-411.

Heaton, T.H., Hall, J.F., Wald, D.J., Halling, M.W. 1995. Response of high-rise and base-isolated buildings to a hypothetical $M_w$ 7.0 blind thrust earthquake. *Science*, 267 (5195), 206-211.

He, W.L., Agrawal, A.K. 2008. An analytical model of ground motion pulses for the design and assessment of smart protective systems. *ASCE journal of structural engineering*, 134 (7), 1177-1188.

Komodromos, P. 2000. *Seismic isolation for earthquake-resistant structures*. WIT Press, 1-85312-803-1.

Mazza, F. & Vulcano, A. 2009. Nonlinear response of RC framed buildings with isolation and supplemental damping at the base subjected to near-fault earthquakes. *Journal of earthquake engineering*, 13 (5), 690-715.

Naeim, F. & Kelly, J.M. 1999. *Design of seismic isolated structures: from theory to practice*. John Wiley & Sons, New York, 978-0-471-14921-7.

Nagarajaiah, S., Reinhorn, A.M., Constantinou, M.C. 1991. 3D-BASIS nonlinear dynamic analysis of three-dimensional base isolated structures: part II. *Technical report NCEER-91-0005*. National centre for earthquake engineering research, State University of New York at Buffalo.

Providakis, C.P. 2008. Effect of LRB isolators and supplemental viscous dampers on seismic isolated buildings under near-fault excitations. *Engineering structures*, 30, 1187-1198.

Providakis, C.P. 2009. Effect of supplemental damping on LRB and FPS seismic isolators under near-fault ground motions. *Soil dynamics and earthquake engineering*, 29, 80-90.

Sommerville, P.G. 1998. Development of an improved representation of near-fault ground motions. *SMIP98 Proceedings, Seminar on Utilization of Strong-Motion Data*, Oakland, CA, September 15, California Division of Mines and Geology, Sacramento, CA, 1-20.

Tsopelas, P.C., Constantinou, M.C., Reinhorn, A.M. 1994. 3D-BASIS-ME: Computer program for nonlinear dynamic analysis of seismically isolated single and multiple structures and liquid storage tanks. *Technical report NCEER-94-0010*. NCEER, State University of New York at Buffalo.